A TRANSIENT NEUTRONIC-THERMALHYDRAULIC COUPLED MODELLING APPROACH

Majid Fassi Fehri, Richard Chambon and Alberto Teyssedou*

Nuclear Engineering Institute, Engineering Physics Department
École Polytechnique de Montréal
C.P. 6079, Succ. Centre-ville
Montréal (Québec), CANADA H3C3A7
(majid.fassi-fehri@polymtl.ca, richard-pierre.chambon@polymtl.ca
alberto.teyssedou@polymtl.ca)

ABSTRACT

Simulating two-phase flow and forced-convection boiling heat transfer constitute important aspects in performing nuclear power-reactor safety analysis. In this work, a transient thermalhydraulic code named ARTHUR (Advanced Routines of Thermal-Hydraulics for Unsteady-states Reactors) was developed and coupled to an existing neutronic code, DONJON-3. To this aim, the flow equations based on the drift-flux model were discretised using a second-order finite-difference for the space domain and a first-order fully implicit method for the time. The flow model has been validated by comparing the simulations with experimental boiling two-phase flow data obtained in uniformly heated tubes. Also, the heat transfer equations for the central pin were discretised using the same discretisation scheme and the model was validated by comparing the simulations with analytical solutions. Finally, coupled neutronic-thermalhydraulic simulations of a simplified CANDU four-channel reactor have been done for several transient conditions.

I. INTRODUCTION

The safety analysis of nuclear power plants requires coupled neutronic-thermalhydraulic calculations. For CANDU systems, coupled neutronic-thermalhydraulic simulations presently use a simplified model with up to 10 representative thermalhydraulic channels. It is elusive, from a logistical view point, to perform thermalhydraulic simulations of channels, without linking them to their neutronic counterparts. Therefore, in this work we achieve channel-by-channel simulation in parallel to a neutronic code. The thermalhydraulic calculations are carried out for the central pin of all 12 contiguous 37-pin fuel bundles and it is assumed that for each axial location in the fuel channels, the flow conditions around are the same as those prevailing for the central pin. This consideration reduces the computational power required for transient calculations and permits us to explore feedback effects between the neutron flux distribution and the thermalhydraulic properties under such conditions. In a first step, we will describe the thermalhydraulic ARTHUR code. Both flow and thermal parts of the code are validated by comparing simulation results with experimental or analytical data. Then, the coupling of ARTHUR with the neutronic code DONJON-3 is described and the results of coupled transient simulations are presented.

II. TWO-PHASE FLOWS MODEL

We consider first two-phase flow conservation equations based on the drift-flux

* Corresponding author: A. Teyssedou, e-mail alberto.teyssedou@polymtl.ca

model [1]; they are written as follows:

$$\frac{\partial \rho_m}{\partial t} + \frac{\partial G}{\partial z} = 0 \quad , \tag{1}$$

$$\frac{\partial G}{\partial t} + \frac{\partial}{\partial z}\left(\frac{G^2}{\rho_m} - \frac{\varepsilon}{1-\varepsilon}\frac{\rho_l \rho_g}{\rho_m}\bar{v}_{gj}^{\,2}\right) + \frac{\partial p}{\partial z} + \rho_m g\cos(\theta) + \left(\frac{\partial p}{\partial z}\right)_{friction} = 0\,, \tag{2}$$

$$\begin{aligned} &\frac{\partial}{\partial t}\left(\rho_m h_m + \frac{G^2}{\rho_M} - p + \rho_m g z\cos(\theta)\right) + \\ &\frac{\partial}{\partial z}\left(G h_m + \varepsilon\frac{\rho_l \rho_g}{\rho_m}\bar{v}_{gj}\Delta h_{\mathrm{lg}} + \frac{G^3}{2\rho_E^2} + Ggz\cos(\theta)\right) = \frac{A_w q''}{V} \end{aligned} \quad . \tag{3}$$

To complete the system of equations, we used Saha-Zuber [2] model to determine the flow quality and the void fraction in the subcooled boiling region, the Müller-Steinhaggen [3] correlation is used to determine two-phase frictional pressure losses while the Chexal-Lellouche [4] correlation is applied in order to calculate the two-phase flow distribution coefficient and the drift velocity. The equations are written in numerical form by using a second-order finite-difference discretisation for the space domain and a first-order fully implicit discretisation for the time. The thermophysical properties the water (coolant) are calculated with the IAPWS-97IF formulation [5].

This portion of the code (i.e., thermalhydraulic model alone) was validated by comparing the simulations with data obtained from experiments carried out in vertical round uniformly heated tubes [6]. Figure 1 shows the comparison of the simulations with single-phase flow data.

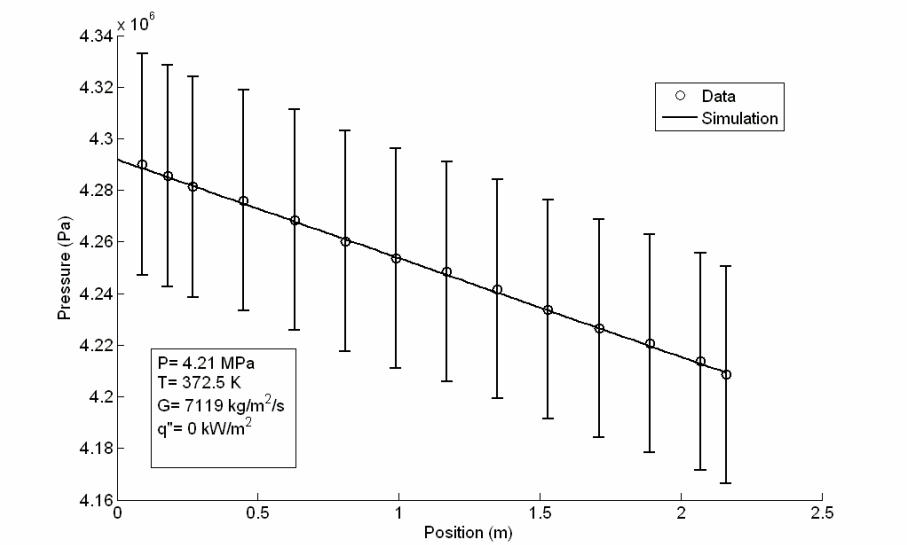

Figure 1. Comparison of simulated vs. measured pressure drop under single-phase flow conditions [6].

For an axial location of 2.16 *m* there is a very small difference that is due to the discretisation scheme. In fact, the total length of the tube is subdivided in *N* nodes while the measured data at 2.16 *m* corresponds to a location *N+1*. Despite this observation, the relative error is less than 1%. We have also compared the predictions of the code with single-phase

flow data obtained for a large range of flow conditions. In all the cases the code predicted the pressure within the experimental error band.

In addition, the thermalhydraulic module of ARTHUR code was also validated against two-phase boiling water data. Figures 2 to 4 present two-phase flow simulations for a typical experiment given in [6]. It must be pointed out that the aforementioned validation procedure was carried out by covering a large range of experimental conditions; however, only one of these simulations is presented in the paper.

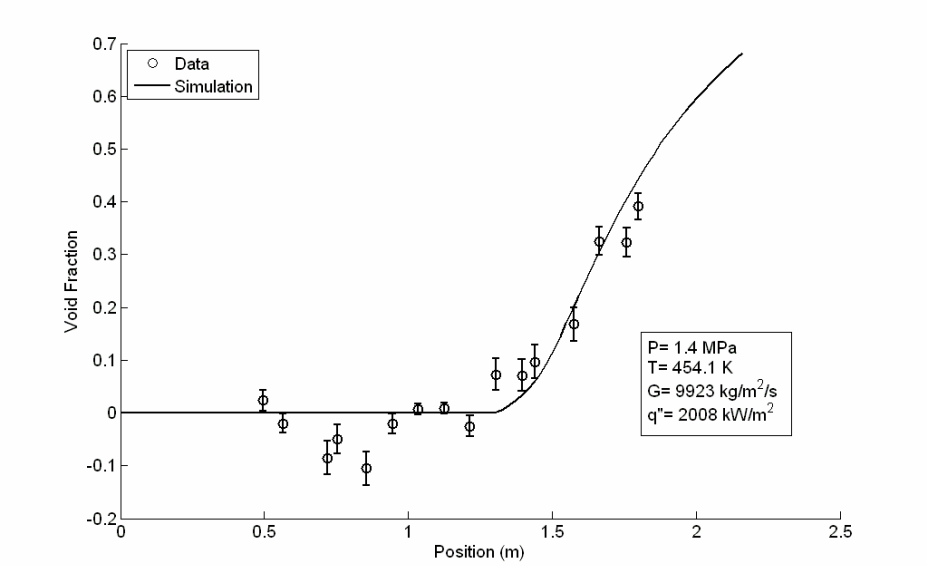

Figure 2: Axial void fraction distributions vs. data given in [6].

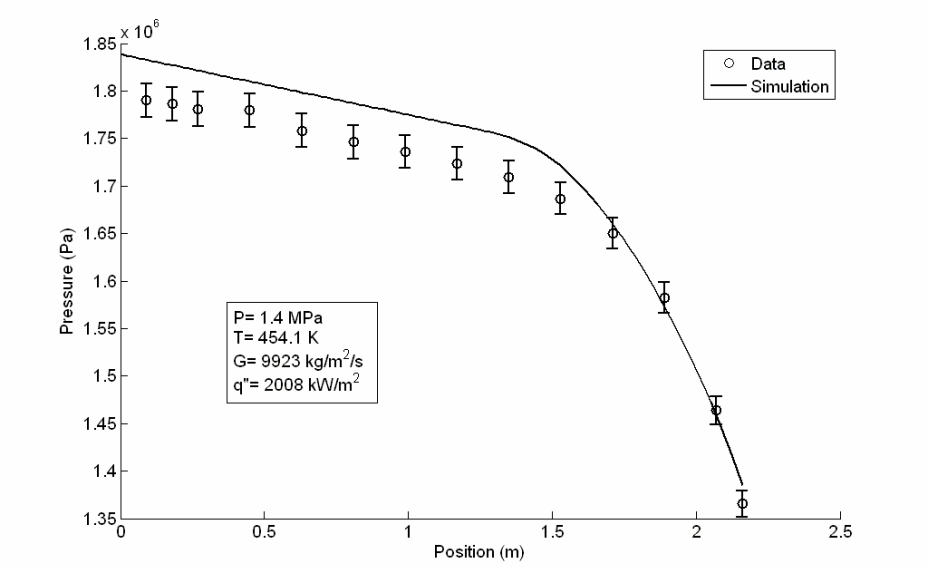

Figure 3: Axial pressure drop profile vs. data given in [6].

Figure 2 shows that in general the code is able to predict the axial void fraction distributions quite well. Further, Figure 4 shows predicted thermodynamic and flow qualities.

A comparison between Figures 2 and 4 clearly indicates that the flow quality profile confirms the void fraction trends, i.e., a void fraction inflection is observed to occur at a distance of about 1.3 m that corresponds to the location where the flow quality starts increasing. Even though the void fraction seems to be correctly predicted, the same cannot be said with respect to the pressure drop. Figure 3 shows that the thermalhydraulic model tends to overestimate the pressure drop. This behaviour has been observed in several experiments we have simulated. In particular, for the case shown in Figure 3, a relative error of 8% between predicted and measured values is observed. This error, nevertheless, is still quite small for a thermalhydraulic calculation. The comparisons carried out for a large range of flow conditions permitted us to validate the proposed model to handle two-phase flows under both subcooled and saturated boiling flow conditions.

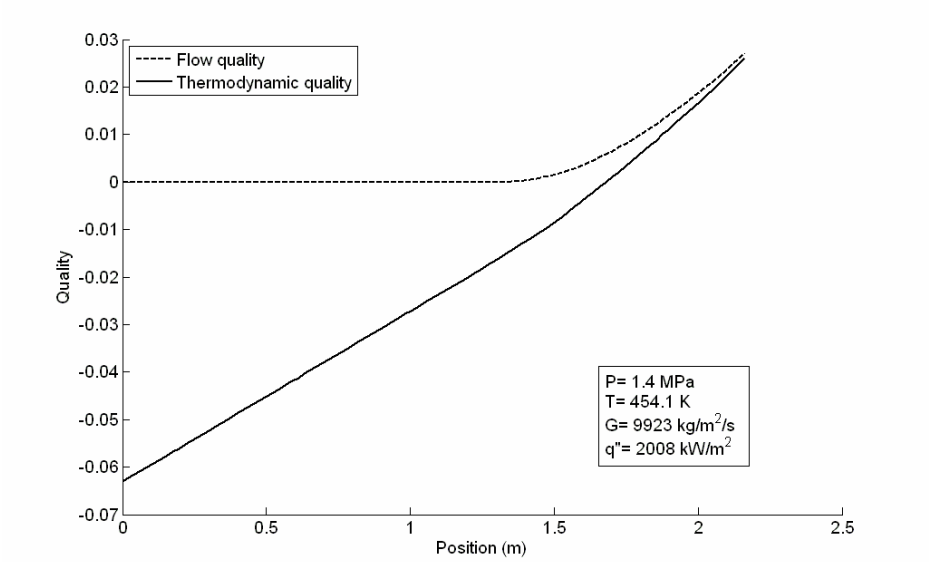

Figure 4: Calculated thermodynamic and flow qualities.

The use of one-dimensional two-phase flow equations, however, revealed a major incoherence in the drift-flux model itself. Figure 5 shows the results obtained from the energy conservation equation. This figure clearly indicates that for a given pressure condition the enthalpy of the liquid phase, calculated according to its definition, can be higher than the enthalpy of the saturated liquid at the same pressure. It is quite possible that this incongruence is caused by the fact that the flow quality, and consequently the void fraction, based on the definition to the flow enthalpy does not necessarily corresponds to the value calculated from the empirical correlations used as a closure relationship. In other terms, the flow quality is obtained from an arbitrary function while it should be given by a model that must rigorously satisfy the actual form of the energy conservation equation. It must be pointed out that this problem has been also observed by other authors [7] who suggest using a modified form of the mass conservation equation to calculate a velocity field that counterbalance this major drawback. However, the proposed equations are not useful for solving transient two-phase flow problems. To partially circumvent this difficulty, in the present work the enthalpy of the liquid phase is used until saturation is reached, afterwards saturation conditions are assumed. It must be mentioned that this assumption does not necessary satisfy the conditions under which most subcooled boiling models were developed. As a matter of fact, in most of the cases researchers suggest using liquid under saturation even though the local liquid

temperature is much lower.

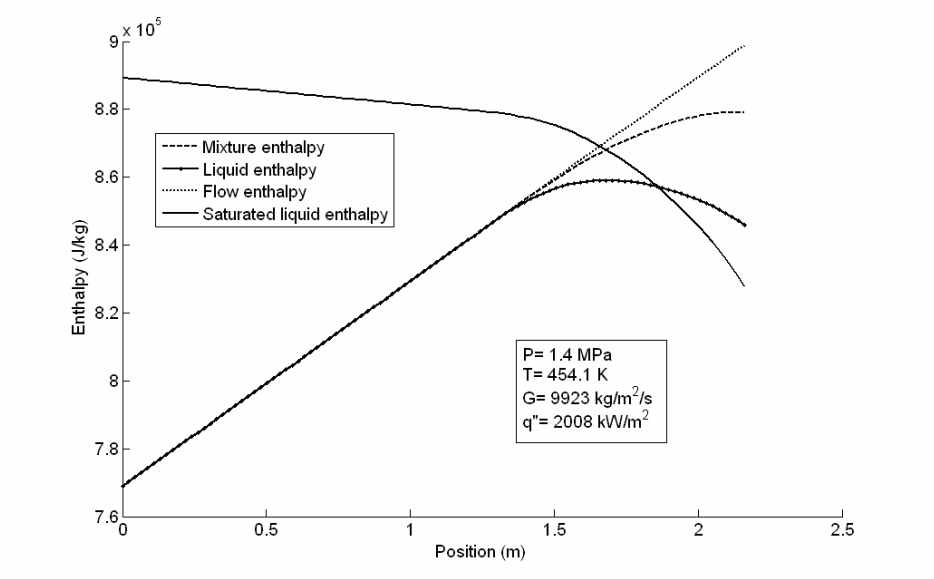

Figure 5: Flow and mixture enthalpy.

III. HEAT TRANSFER MODEL

A radial heat-transfer model for the cladding and fuel pellets was also included in the code. This model permits the temperature distribution in the pins to be determined. The heat transfer equation is written as:

$$\frac{\partial \rho C_p T}{\partial t} = \frac{k}{r}\frac{\partial}{\partial r}\left(\frac{\partial T}{\partial r}\right) + q''' \quad . \tag{4}$$

This equation is discretised by applying the same scheme used for coding the two-phase flow model discussed above. In order to close the system of equations, we have included the following relationships: Markoczy [8] and Chen [9] correlations are used for calculating the forced convection heat-transfer coefficient between cladding and the coolant for single- and two-phase flow respectively. Furthermore, the heat-transfer across the gap between fuel and clad is modeled as:

$$k_c \left.\frac{\partial T}{\partial r}\right|_{r=rc} \approx h_{gap}\left(T_f - T_c\right). \tag{5}$$

Where a constant thermal conductance of 10 kW/Km^2 is assumed. Furthermore, the validation of the heat transfer across the fuel pin was validated against a simplified analytical solution of a pin of a typical 37-element bundle under the conditions specified in Table 1. The comparison of the simulations with the analytical solution of the heat transfer equation is shown in Figure 6. The difference between the two solutions is quite possible due to the relatively coarse discretisation we have applied to the cladding. However, the overall error is lower than 2% therefore we consider that the proposed modelling approach is acceptable for treating more complex cases, i.e., fuel pin subjected to axial heat flux distributions. To treat such a case, and considering that the thermal conductivities are affected by the local fuel

temperature, the thermophysical properties for both the cladding and the Uranium oxide are calculated using the equations recommended by the IAEA [10].

Table 1. Conditions used for obtaining the analytical heat transfer solution .

Uniform power density (GW/m^3)	0.3
Fuel radius (mm)	5.6
Internal clad radius (mm)	6.14
External clad radius (mm)	6.52
Thermal conductivity of the fuel (W/mK)	5.0
Thermal conductivity of the clad (W/mK)	10.0
Heat transfer coefficient in the gap (kW/m^2K)	10.0
Temperature at the surface of the clad (K)	541.8

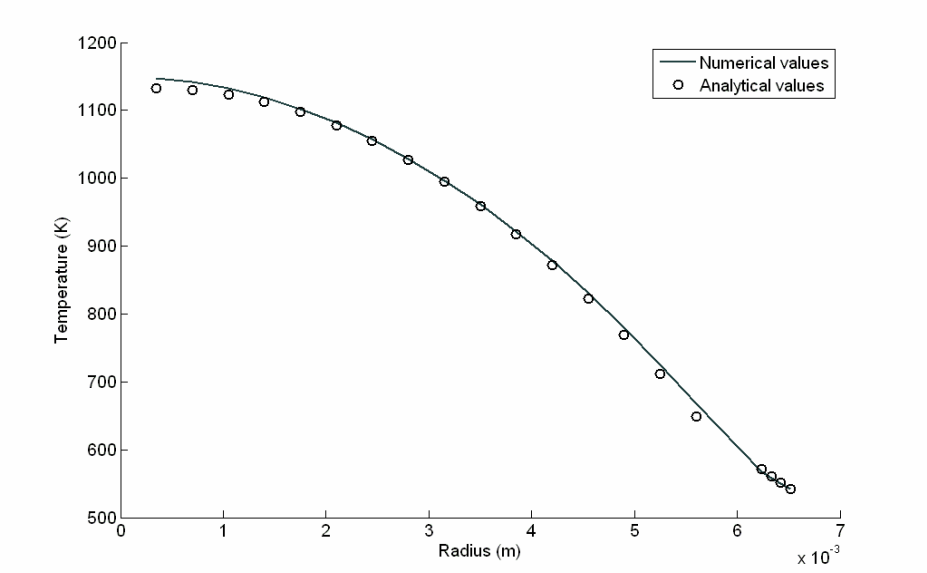

Figure 6. Radial temperature distribution in a typical fuel pin.

IV. COUPLED NEUTRONIC/THERMALHYDRAULIC SIMULATIONS

A four-channel CANDU-6 nuclear core is simulated under transient conditions. Figure 7 shows the algorithm used to solve the thermalhydraulic and the heat transfer models. Herewith, a single convergence criterion of 10^{-6} is used for conducting all the simulations presented in this paper. To simulate transient conditions the following flow parameters were sequentially varied: inlet channel mass flow rate, coolant inlet subcooling and outlet pressure. The simulations are carried out by considering nominal reactor operation values as initial conditions; they are summarized in Table 2, and the transient conditions used to perform each simulation are given in Table 3.

The thermalhydraulic and heat transfer models were coupled to the neutronics code DONJON-3 [11,12,13,14]. Figure 8 shows the algorithm used for carrying out coupled calculations. A convergence criterion of 10^{-4} is used to perform neutronic calculations. The cross-sections of the pellets and the coolant are evaluated as a function of the local

temperature by using the FeedBack Model [15]. It is obvious that the effects of coolant density changes (i.e., void fraction) are implicitly taken into account.

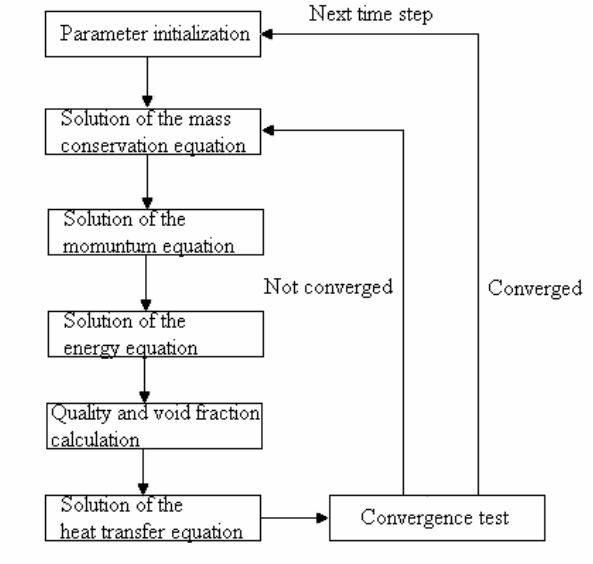

Figure 7. ARTHUR's thermal calculation algorithm.

Table 2. Four-channel CANDU-6 nominal operation conditions.

Total power (*MW*)	21.7
Inlet coolant temperature (*K*)	535.5
Outlet coolant pressure (*MPa*)	11.2
Inlet coolant mass flow (kg/m^2s)	7007.8

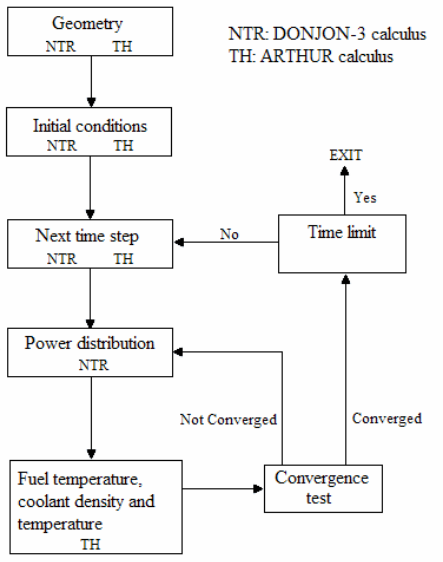

Figure 8. Coupled neutronic/thermalhydraulic calculation algorithm.

Table 3: Thermalhydraulic transient conditions.

Case 1 : Variation rate of the inlet mass flux	-4.3%/*min*
Case 2 : Variation rate of the inlet coolant temperature	0.6%/*min*
Case 3 : Variation rate of the outlet pressure	-5.0%/*min*

The simulations of the effects of a decrease in the inlet mass flow rate are shown in Figure 9. It is obvious that the bulk coolant temperature increases and the coolant density decreases with decreasing the inlet mass flow rate. The increase in the coolant temperature provokes an increase on the average fuel temperature. The combined effect of these variations causes a positive reactivity change (i.e., strong positive reactivity due to a lower coolant density which is not compensated by a possible minor negative reactivity associated with the increase on the fuel and coolant temperatures) that triggers an increase on power. The results given in Figure 9 clearly show that the neutronic feedback, i.e., the nuclear power increase caused by the positive reactivity, somewhat tends to amplify the variations of thermalhydraulic variables that in turn contribute to accentuate the positive feedback process.

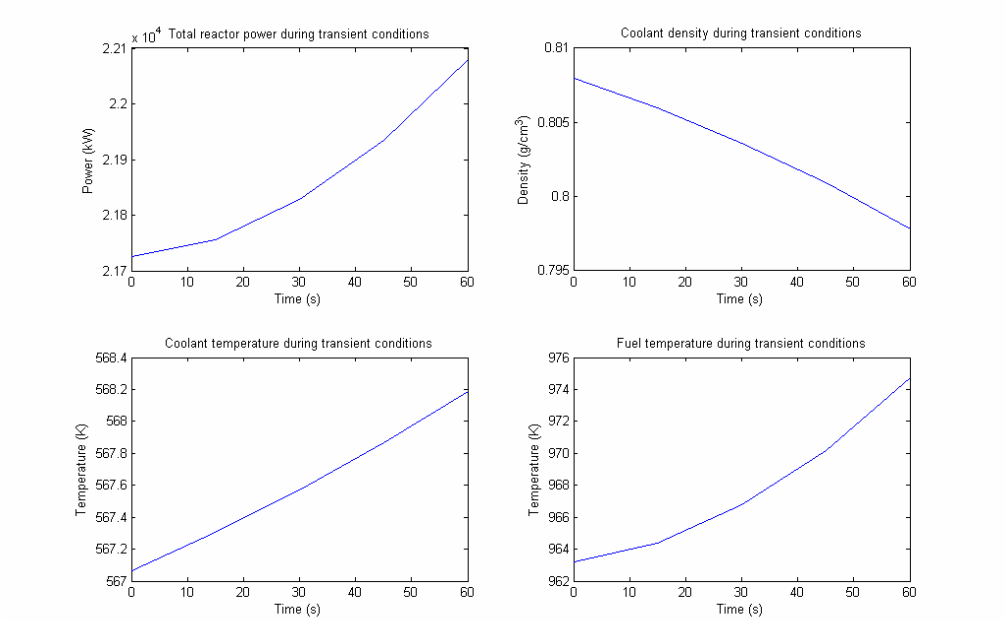

Figure 9. Transient simulations for a decrease of the inlet mass flow rate.

Figure 10 shows the effect of a decrease on the inlet subcooling. Increasing the inlet coolant temperature brings about an increase of the average fuel temperature and a decrease on the coolant density. Similar to the former case, these thermalhydraulic variations provoke a positive reactivity change, i.e., the power increases. It is once again observed that feedback effects tend to destabilize the reactor (i.e., there is a net thermalhydraulic/neutronic positive feedback).

Finally, Figure 11 shows the results obtained when the outlet pressure is forced to decrease. Such a decrease causes both the bulk coolant temperature and density to decrease. These thermalhydraulic variations bring about an increase of the average fuel temperature because there is a strong positive reactivity variation. In turn, this change in reactivity

provokes an increase in the power causing the fuel average temperature to increase. This result is in opposition to what it should be expected. Thus, coupling thermalhydraulics with neutronics calculations clearly shows that the combined effects of fuel and coolant temperature, and density may bring about coupled feedback modes that are not necessarily intuitive.

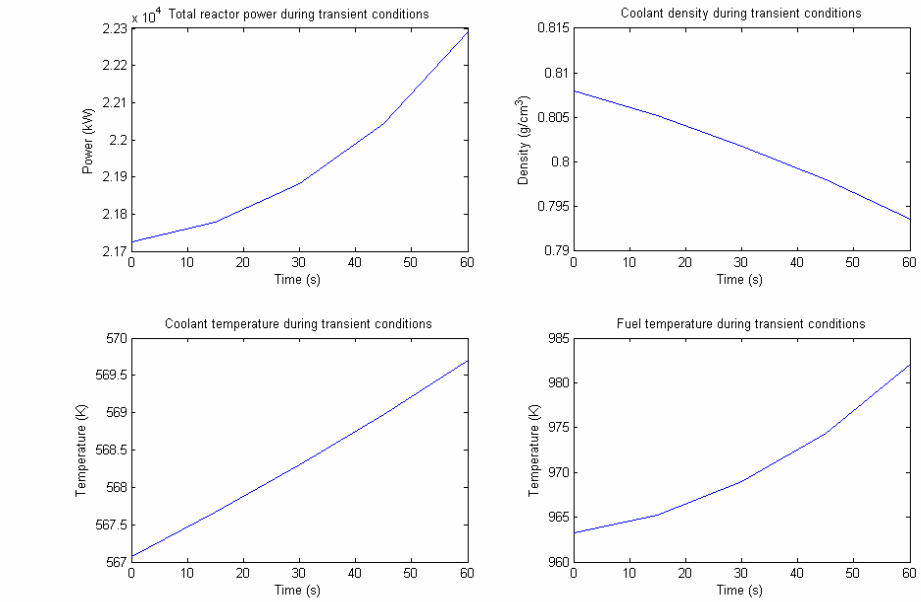

Figure 11. Transient simulations for a decrease of the inlet subcooling.

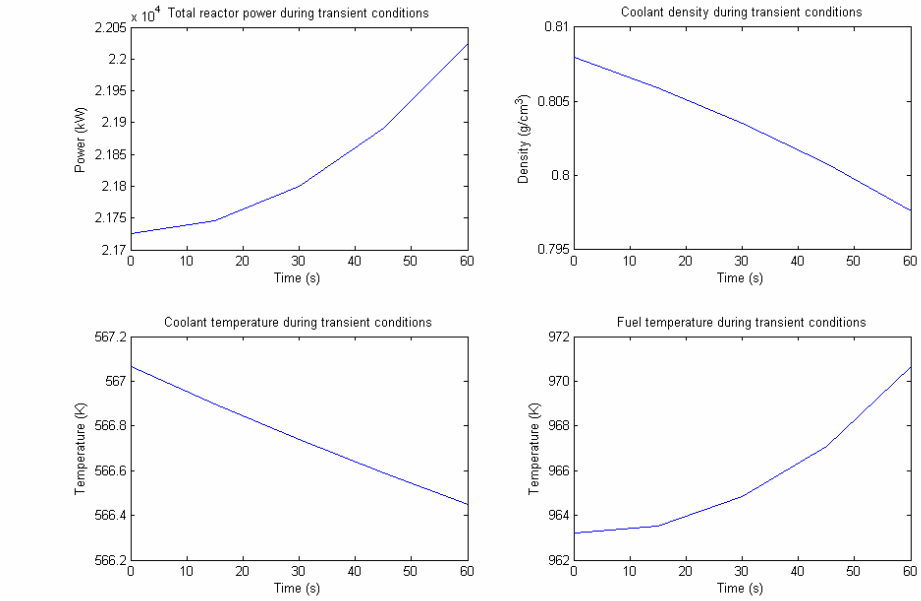

Figure 10. Transient simulations for outlet pressure decrease.

It must be pointed out, however, that the present model does not include critical heat flux evaluation procedures; therefore, it is assumed that the thermahydraulic changes do not

affect the heat transfer conditions to the coolant other than those due to the variation of fluid properties in the convection heat transfer relationships.

As expected, the analysis presented in this section show that coolant density has a higher impact on reactivity than the coolant and fuel temperatures. Even though a rigorous analysis necessitates the study of the behaviour of the cross-sections as function of temperatures, these simulations indicate that both the reactor power and average fuel temperature are mostly determined by the coolant density conditions prevailing in the channel.

V. CONCLUSIONS

In this work, a thermalhydraulic code, ARTHUR was developed based on the idea that the flow conditions at each axial location in a channel can be determined as a function of the conditions prevailing in a central pin of the bundle. The thermalhydraulic calculations were validated against experimental data obtained in vertical uniformly heated tubes. The heat transfer model was validated by comparing the results with simplified analytical solutions. The use of dimensional conservation equations, however, revealed that the drift-flux model is not able to completely respect the conservation of energy. Coupling calculations using ARTHUR with the neutronic code DONJON-3 permitted important feedback effects to be observed. In particular, it seems that the reactivity is affected by coolant density changes rather than by temperature effects.

ACKNOWLEDGMENTS

We strongly appreciate the help of Mr. Alexi Popov. This work was funded by the Hydro-Québec chair in nuclear engineering and by the NSERC discovery grant # RGPIN 41929.

REFERENCES

[1] M. Ishii and T. Hibiki, *Thermo-Fluid Dynamics of Two-Phase Flow*. New York, Springer, 2006.

[2] P. Saha and N. Zuber, "Point of Net Vapour Generation And Vapour Void Fraction In Subcooled Boiling," *Muanyag Es Gumi,* pp. 175-179, 1974.

[3] H. Müeller-Steinhagen and K. Heck, "Simple Friction Pressure Drop Correlation For Two-Phase Flow In Pipes," *Chemical Engineering and Processing,* vol. 20, pp. 297-308, 1986.

[4] B. Chexal, G. Lellouche, J. Horowitz, and J. Healzer, "A Void Fraction Correlation For Generalized Applications," *Progress in Nuclear Energy,* vol. 27, pp. 255-95, 1992.

[5] W. Wagner, J. R. Cooper, A. Dittmann, J. Kijima, H. J. Kretzschmar, A. Kruse, R. Mares, K. Oguchi, H. Sato, I. Stocker, O. Sifner, Y. Takaishi, I. Tanishita, J. Trubenbach, and T. Willkommen, "The IAPWS Industrial Formulation 1997 For The Thermodynamic Properties Of Water And Steam," *Journal of Engineering for Gas Turbines and Power,* vol. 122, pp. 150-180, 2000.

[6] F. Aube, «Effets du flux de chaleur sur les pertes de pression par frottement dans des ecoulements monophasiques et diphasiques», Ph.D. Thesis, Ecole Polytechnique, Montréal, 1996.

[7] F. J. Collado, C. Monné and A. Pascau, "A New Heat Balance for Flow Boiling," *AIChE Journal,* vol. 53(8), pp. 2123-2130, 2007.

[8] G. Markoczy, "Convective Heat Transfer in Rod Clusters with Turbulent Axial Coolant Flow, Part I : Mean Values over the Rod Perimeter," *Wärme und Stoffübertragung*, vol. 5, pp. 204-212, 1972.

[9] J. C. Chen, "Correlation For Boiling Heat Transfer To Saturated Fluids In Convective Flow," *Industrial and Engineering Chemistry - Process Design and Development,* vol. 5, pp. 322-329, 1966.

[10] IAEA, *Thermophysical Properties Database Of Materials For Light Water Reactors And Heavy Water Reactors*, Report IAEA-TECDOC-1496, AIEA, June, 2006.

[11] E. Varin and A. Hébert, *Data Structures of DONJON-3*, Report IGE-226, Institut de Génie Nucléaire, École Polytechnique de Montréal, November, 2003.

[12] E. Varin, A. Hébert, R. Roy and J. Koclas, *A User Guide for DONJON-3*, Report IGE-208, Institut de Génie Nucléaire, École Polytechnique de Montréal, August, 2005.

[13] R. Roy and A. Hébert, *The GAN Generalized Driver*, Report IGE-158, Institut de Génie Nucléaire, École Polytechnique de Montréal, March, 2000.

[14] R. Roy, *The CLE-2000 Tool-Box*, Report IGE-163, Institut de Génie Nucléaire, École Polytechnique de Montréal, December, 1999.

[15] M. T. Sissaoui, G. Marleau, and D. Rozon, "CANDU Reactor Simulations Using The Feedback Model With Actinide Burnup History," *Nuclear Technology,* vol. 125, pp. 197-212, 1999.